Environmental Science & Technology

Article

pubs.acs.org/est

Comparison of Particle Mass and Solid Particle Number (SPN) Emissions from a Heavy-Duty Diesel Vehicle under On-Road Driving Conditions and a Standard Testing Cycle

Zhongqing Zheng,[†,‡] Thomas D. Durbin,[‡] Jian Xue,[†,‡] Kent C. Johnson,[‡] Yang Li,[†,‡] Shaohua Hu,[§] Tao Huai,[§] Alberto Ayala,[§] David B. Kittelson,[∥] and Heejung S. Jung*[,†,‡]

[†]Department of Mechanical Engineering, and [‡]Center for Environmental Research and Technology (CE-CERT), College of Engineering, University of California Riverside, Riverside, California 92521, United States

[§]Monitoring and Laboratory Division, California Air Resources Board (CARB), Sacramento, California 95814, United States

[∥]Department of Mechanical Engineering, University of Minnesota, 111 Church Street Southeast, Minneapolis, Minnesota 55455, United States

Supporting Information

ABSTRACT: It is important to understand the differences between emissions from standard laboratory testing cycles and those from actual on-road driving conditions, especially for solid particle number (SPN) emissions now being regulated in Europe. This study compared particle mass and SPN emissions from a heavy-duty diesel vehicle operating over the urban dynamometer driving schedule (UDDS) and actual on-road driving conditions. Particle mass emissions were calculated using the integrated particle size distribution (IPSD) method and called M_{IPSD}. The M_{IPSD} emissions for the UDDS and on-road tests were more than 6 times lower than the U.S. 2007 heavy-duty particulate matter (PM) mass standard. The M_{IPSD} emissions for the UDDS fell between those for the on-road uphill and downhill driving. SPN and M_{IPSD} measurements were dominated by nucleation particles for the UDDS and uphill driving and by accumulation mode particles for cruise and downhill driving. The SPN emissions were ~3 times lower than the Euro 6 heavy-duty SPN limit for the UDDS and downhill driving and ~4−5 times higher than the Euro 6 SPN limit for the more aggressive uphill driving; however, it is likely that most of the "solid" particles measured under these conditions were associated with a combination release of stored sulfates and enhanced sulfate formation associated with high exhaust temperatures, leading to growth of volatile particles into the solid particle counting range above 23 nm. Except for these conditions, a linear relationship was found between SPN and accumulation mode M_{IPSD}. The coefficient of variation (COV) of SPN emissions of particles >23 nm ranged from 8 to 26% for the UDDS and on-road tests.

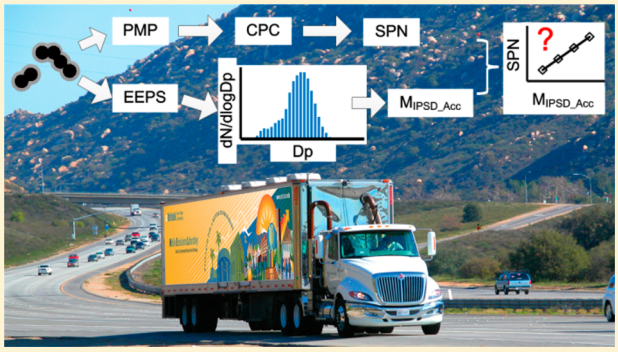

1. INTRODUCTION

Diesel exhaust particles are known to have adverse effects to human health.[1] The traditional mass-based particulate matter (PM) measurement method has been shown to have issues with sensitivity as PM regulations have become more stringent. A solid particle number (SPN)-based measurement method has been developed in Europe[2] to complement gravimetric mass measurements. The SPN measurement protocol was developed through the Particle Measurement Programme (PMP). The European Union has implemented a solid particle number (SPN) standard for both light- and heavy-duty diesel vehicles. They have also been discussing the regulation of SPN emissions for other sectors (e.g., aviation and off-road).[3] The PMP protocol measures solid particles using a PN counter with a counting efficiency being 50 ± 12% at 23 nm and rising to >90% at 41 nm, where solid particles are operationally defined as particles that remain after passing through an evaporation tube that has a wall temperature of 300−400 °C.[4] Note that the SPN emissions described in this paper are defined on the basis of the PMP definition for SPN emissions.

The PMP measurement protocol has been intensively tested under laboratory conditions, and the repeatability (20−61%) and reproducibility (30−80%) for this protocol have been found to be better than those for gravimetric PM mass for both light- and heavy-duty diesel engines.[2,5] However, several studies have shown that a significant number of sub-23 nm particles can be present downstream of the PMP system.[6−8] Various experiments have been conducted to investigate the nature of these sub-23 nm particles. Zheng et al.[9] showed that most of

Received: August 16, 2013
Revised: November 29, 2013
Accepted: December 13, 2013
Published: December 13, 2013

the sub-23 nm particles downstream of the PMP system were formed through renucleation of semi-volatiles. Their conclusion was based on comparisons that they made between a PMP system and a catalytic stripper system using laboratory-generated aerosols composed of sulfuric acid and hydrocarbons and using diesel exhaust from a heavy-duty vehicle at steady-state conditions. In another study, Zheng et al.[10] also concluded that the majority of the sub-23 nm particles downstream of the PMP system were renucleated semi-volatiles by comparing the sub- and super-23 nm PN concentrations at different PMP dilution ratios over the heavy-duty urban dynamometer driving schedule (UDDS). It was also found in both studies[9,10] that there were negligible particles between 10 and 23 nm downstream of the PMP system; i.e., the renucleated particles were smaller than 10 nm.

In Europe, SPN emissions are measured under the same test cycles as PM mass emissions and other gaseous emissions.[11,12] For heavy-duty engines, cycles, such as the world harmonized steady cycle (WHSC) and the world harmonized transient cycle (WHTC), will be used to evaluate SPN for regulatory requirements starting with the Euro 6 standards. These test cycles were designed to represent on-road driving emission levels. It is uncertain whether laboratory test cycles reflect on-road driving conditions, especially for the newly regulated SPN emissions. Currently, there is no SPN regulation in the United States. In the Zheng et al.[10] study, a very high level of particles larger than 23 nm particles was reported downstream of a PMP system under an aggressive on-road, flow-of-traffic driving condition. In that study, however, the elevated engine load, on-road, flow-of-traffic driving was performed only once. Therefore, no statistical comparisons could be made.

In-use testing of diesel engine emissions has gained increasing attention in the past few years worldwide. Portable emission measurement systems (PEMSs) are required to measure in-use emissions for both gaseous and PM mass emissions. In Europe, after the establishment of the Euro 5 and Euro 6 SPN standards for both light- and heavy-duty diesel engines, there are ongoing discussions about regulating in-use SPN emissions from diesel engines. Good correlations between PEMS measurements and laboratory constant volume sampling (CVS) measurements are one of the key factors to ensure the accuracy of PEMS measurement. Such correlation studies have been carried out under controlled laboratory conditions for PM[13] and over on-road driving conditions for both gaseous and PM PEMSs.[14,15] It is also of interest to investigate the behavior of SPN emissions under on-road driving conditions.

This study examined particle mass and SPN emissions from a heavy-duty diesel vehicle equipped with a Johnson Matthey continuously regenerating trap (CRT) over well-designed, on-road driving conditions and a standard testing cycle, the UDDS. The main objective of this study is to address how particle mass and SPN emissions vary over on-road driving conditions and a standard testing cycle. The changes in PN emissions for particles both smaller and larger than 23 nm were characterized for different driving conditions in this paper. Additionally, the integrated particle size distribution (IPSD) method was used to calculate a particle mass (M_{IPSD}) using particle size distributions.

2. EXPERIMENTAL APPROACH AND CALCULATION PROCEDURE

2.1. Measurement Setup. Figure 1 shows a schematic of the measurement system. All instruments were installed inside

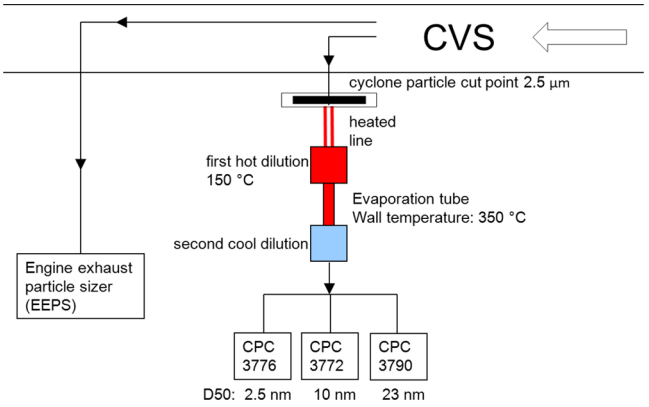

Figure 1. Schematic diagram of the testing arrangement for the on-road and UDDS tests. The APC is the first part of the sampling system below the cyclone consisting of the first stage of hot dilution, an evaporation tube, a second stage of cool dilution, and CPC 3790. CPC 3776 and CPC 3772 are connected to the output of secondary cool dilution.

the University of California Riverside (UCR), College of Engineering, Center for Environmental Research and Technology (CE-CERT)'s Mobile Emission Laboratory (MEL).[15] The MEL has a built-in CVS system. The PMP system used in this study was an AVL particle counter advanced (APC, AVL List GmbH). It is a commercially available, PMP-compliant instrument that measures SPN emissions. It consists of a primary hot diluter, an evaporation tube, and a secondary cool diluter. The PMP regulation uses a particle concentration reduction factor (PCRF) to account for both dilution (including primary and secondary dilutions) and particle losses in the entire PMP system.[12] The overall PCRF of the APC is calibrated by the manufacturer in compliance with the UNECE Regulation 83. The overall PCRF used in this study was 500. The heating temperatures of the primary diluter and evaporation tube were 150 and 350 °C, respectively.

Three condensation particle counters (CPCs) with different cutoff diameters (D_{50}) were employed to measure SPN emissions downstream of the PMP system. They were CPC 3790 (D_{50} = 23 nm), CPC 3772 (D_{50} = 10 nm), and CPC 3776 (D_{50} = 2.5 nm). The SPN concentrations downstream of the PMP system presented later in this paper are all corrected for the PMP PCRF. It should be noted that the PMP PCRF is an average value of three monodisperse PCRFs calibrated with 30, 50, and 100 nm particles. Therefore, the PCRF-corrected SPN concentrations downstream of the PMP system may underestimate the actual SPN concentrations upstream of the PMP system.[4] This underestimation is more severe for smaller particles, because smaller particles have greater diffusion losses.

An engine exhaust particle sizer (EEPS, TSI 3090) measured particle number size distributions from 5.6 to 560 nm in the CVS system. M_{IPSD} emissions were calculated from the EEPS particle size distributions, the details of which are discussed later in this paper.

2.2. Test Vehicle, Fuel, and Lubricant. The vehicle and aftertreatment system were the same as that used for the on-road test in previous California Air Resources Board (CARB)/UCR PMP studies.[8,10] The vehicle was a 14.6 L, 2000 Caterpillar C-15 engine equipped, Freightliner class 8 truck. A Johnson Matthey CRT was installed on the vehicle. Kittelson et al.[16] reported 95% of PM reduction when using the CRT. Lanni et al.[17] also reported particle size distributions with and without

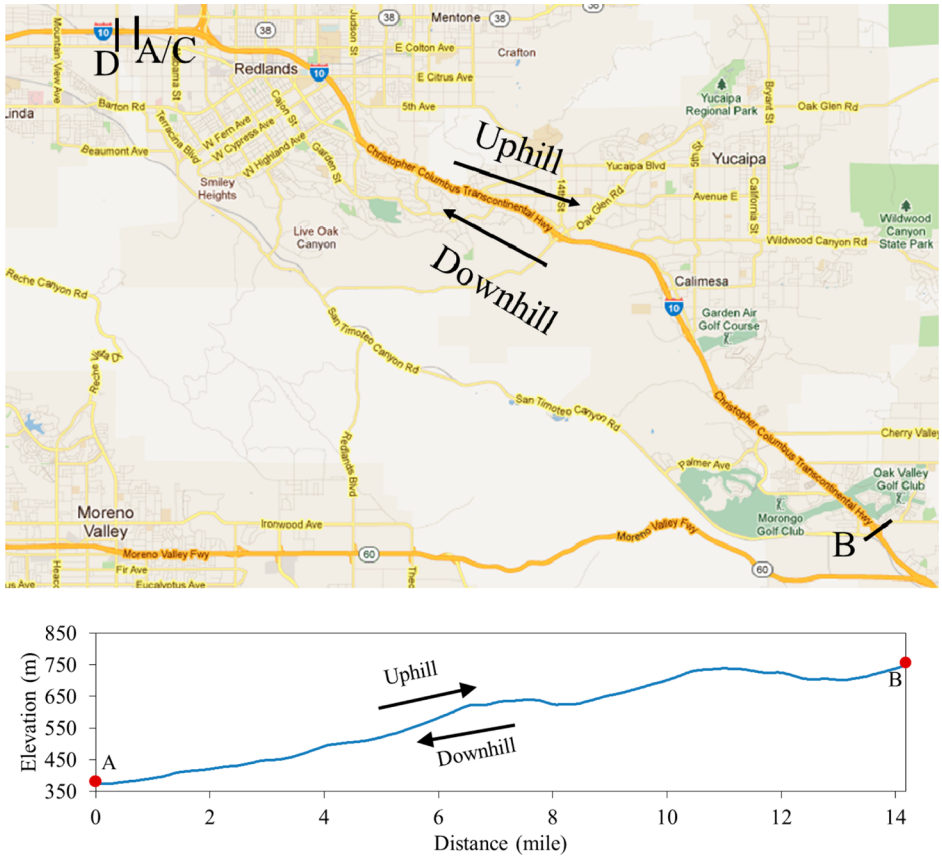

Figure 2. Map and elevation variation of the uphill and downhill driving of the on-road test.

a CRT. They showed above 90% filtration efficiency for accumulation mode particles. The truck and MEL trailer combined have a weight of approximately 65 000 lbs, including all emission instruments. The truck had a mileage of 41 442 miles at the beginning of the testing. CARB ultralow sulfur diesel (ULSD) fuel (8 ppm of sulfur by weight) and standard lubricating oil with a sulfur level of 0.29% were used.

2.3. Test Cycles. The tests were conducted over a standard driving cycle, the UDDS, and three on-road driving conditions (cruise, uphill, and downhill driving), where the truck and MEL are driven in the flow-of-traffic. The UDDS was conducted on CE-CERT's heavy-duty chassis dynamometer and repeated 3 times. The on-road cruise was performed by driving the CE-CERT's MEL at 50−70 miles per hour (mph) on U.S. Interstate-215 (I-215) freeway near Riverside, CA, under flow-of-traffic conditions. The on-road cruise test was conducted only once. The uphill and downhill on-road flow-of-traffic tests were performed over 2 days by driving the CE-CERT's MEL at 45−70 mph on U.S. Interstate-10 (I-10) freeway near Palm Springs, CA (Figure 2). The uphill driving was east bound on I-10. The downhill driving was west bound on I-10 and was the return trip of uphill driving. The overall road grades of uphill and downhill driving routes were about 1.6 and −1.6%, respectively, which were calculated as the ratio of rise to run for each route. As shown in Figure 2, uphill driving began at point A and ended at point B, which is also the turn-around location. Downhill driving began immediately after the ending of uphill driving at point B and ended at point C, about the same longitude and latitude as point A. After the downhill driving was completed, the MEL was turned around at point D to start another repeat. The uphill and downhill on-road flow-of-traffic tests were repeated 4 times. The average wind speed was 5.6 mph over test days, and the wind direction was northwest and west for the majority of time during the first and second test days, respectively.

2.4. PM Mass Emission Calculation. The uphill driving and downhill driving segments were conducted back to back, with no stops between to keep the on-road flow-of-traffic driving continuous, as discussed in the previous section; thus, only one filter sample was taken for each repeat of the on-road test (i.e., including uphill and downhill driving). To compare PM mass emissions for uphill and downhill driving, M_{IPSD} emissions were calculated from the EEPS particle size distributions measured in the CVS, using the IPSD method. The IPSD method calculates total particle mass from measured particle size distributions using eq 1. The IPSD method was introduced by Liu et al.,[18] who showed good agreement between the IPSD and gravimetric filter sample measurements. The IPSD method is less subject to the impacts of artifacts, on the other hand, and can be more representative of the particle mass directly from a particle source. In the discussion of this manuscript, PM mass emissions will be referred to as IPSD PM mass emissions

$$M_{IPSD} = \sum_i \rho_{eff,i}\left(\frac{4}{3}\pi\left(\frac{D_{p,i}}{2}\right)^3\right)n_i \quad (1)$$

where M_{IPSD} is the total suspended particle mass, i is the particle size channel, $\rho_{eff,i}$ is the effective density of particles falling in the size channel i, $D_{p,i}$ is the midparticle diameter of the size channel i, and n_i is the total number of particles in size channel i.

dx.doi.org/10.1021/es403578b | Environ. Sci. Technol. 2014, 48, 1779−1786

The effective density correlation for the accumulation mode (soot) particles was adopted from Maricq and Xu[19] and is defined in eq 2

$$\rho_{\mathrm{eff},i} = \rho_0 \left(\frac{D_{\mathrm{p},i}}{D_{\mathrm{p0e}}} \right)^{d_f - 3} \quad (2)$$

where ρ_0 is the primary particle density, D_{p0e} is the effective primary particle diameter, and d_f is the fractal dimension. Values of ρ_0, D_{p0e}, and d_f were 2 g/cm^3, 16 nm, and 2.35, respectively. The accumulation mode particles were chosen to be particles larger than 30 nm, which is typically the cut point between the nucleation mode and accumulation mode defined by Kittelson et al.[20] Ristimäki et al.[21] reported particle effective density for heavy-duty engine exhaust particles. Their results agreed well with that for medium-duty diesel engines reported by Park et al.[22] and that for light-duty diesel engines reported by Maricq and Xu.[19] Both Liu et al.[18] and our study applied the results by Maricq and Xu[19] to the heavy-duty diesel engine exhaust particles. Maricq and Xu[19] estimated that the uncertainty in the mass calculated from particle size distributions is roughly 25%. Particle effective density can change as a function of engine operating conditions, and there are ongoing efforts to determine particle effective densities more appropriate for transient cycles for light-duty vehicles. This follow-up work will be presented as a separate paper. For the nucleation mode particles, a density of 1.46 g/cm^3 was used,[9] assuming that the nucleation mode consists of spherical hydrated sulfuric acid particles with a density of 1.46 g/cm^3. This is the density of such particles at an ambient relative humidity (25 ± 3%) and temperature (33 ± 1 °C),[23] the conditions for the current study.

3. RESULTS

3.1. Real-Time PN Emissions. Typical real-time PN concentrations downstream of the PMP system are shown in Figure 3 for the UDDS test. Vehicle speed, engine power, and exhaust temperature are also plotted in Figure 3. The CPC 3776_2.5 concentrations were always higher than the concentrations of the other two CPCs, indicating the existence of sub-10 nm particles downstream of the PMP system. CPC 3772_10 tracked closely with CPC 3790_23, indicating a negligible number of particles between 10 and 23 nm present downstream of the PMP system, consistent with our previous study.[10]

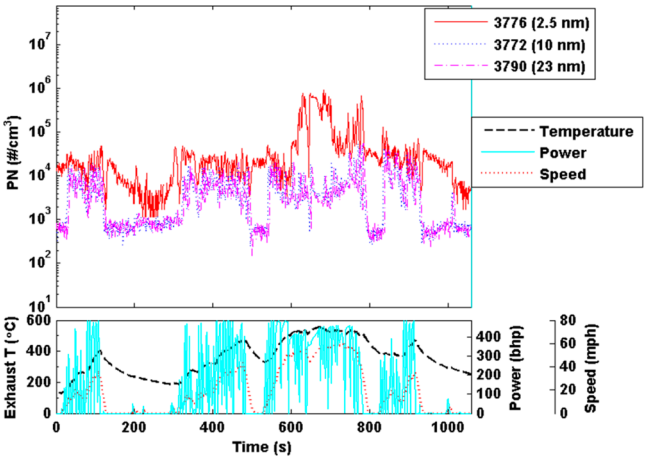

Figure 3. Real-time PN concentrations downstream of the PMP system for the UDDS test.

The previous study[10] found the existence of sub-23 nm particles downstream of the PMP system by comparing particle concentrations using different cutoff diameter CPCs. They also used the catalytic stripper in series with the CPCs to understand the nature of particles. They reported that the majority of these sub-23 nm particles under the PMP system are a result of renucleation of semi-volatile materials. Ntziachristos et al.[24] also confirmed that the sub-23 nm particles below the PMP system are semi-volatile by removing them using a catalytic stripper.

When the concentrations for the two high cutoff diameter CPCs, CPC 3772_10 and CPC 3790_23, were relatively high, the differences between CPC 3776_2.5 and the high cutoff diameter CPCs were generally small. This can be seen during the acceleration periods between 30 and 110 s, between 320 and 490 s, between 540 and 600 s, and between 840 and 920 s. This is due to competition between the processes of nucleation of volatile vapors to form new particles and condensation of volatile vapors onto existing solid soot particles downstream of the PMP system. When more solid soot particles are available (as indicated by the relatively high concentrations of CPC 3772_10 and CPC 3790_23), more condensation onto existing soot particles will occur, resulting in lower volatile vapor concentrations and, hence, less renucleated sub-10 nm particles. This is indicated by the relatively small differences between the CPC 3776_2.5 concentrations and the CPC 3772_10 and CPC 3790_23 concentrations during the time periods indicated above. Between t = 600 and 800 s, the CPC 3776_2.5 concentrations were about 2 orders of magnitude higher than the CPC 3772_10 and CPC 3790_23 concentrations, even when the accumulation soot particle concentrations were relatively high. This same time window was also associated with the highest exhaust temperatures, which led to increased rates of conversion of sulfur in the fuel to sulfuric acid by the catalyzed aftertreament system, as well as possible release of sulfates or other low vapor pressure materials stored in the aftertreatment system at lower temperatures.[25,26] This likely leads to the formation of extremely high semi-volatile vapor concentrations downstream of the PMP system, which, in turn, are associated with very high concentrations of nucleation mode particles in the CVS tunnel, as measured by the EEPS and shown in Figure S1 of the Supporting Information. Kittelson et al.[27] and Herner et al.[28] also found that high exhaust temperatures led to the formation of high concentrations of nucleation mode particles with catalyzed aftertreament systems. PN concentrations of nucleation mode particles (D_p < 30 nm) measured by the EEPS in the CVS during this time window ranged from 8.4 × 10^5 to 3.5 × 10^7 particles/cm^3. Average engine loads and average exhaust temperatures for the on-road and UDDS tests are shown in Figure S2 of the Supporting Information. A comparison between numerically filtered EEPS data and CPC 3790 downstream of the PMP system was performed in a previously published paper[9] to compare the EEPS to a CPC to estimate the uncertainty on the absolute level. The comparison showed that the two instruments agree within 20 ± 11% (see their Figure 6b).

Figure 4 shows the real-time PN concentrations downstream of the PMP system for the on-road, flow-of-traffic uphill and downhill driving tests. Elevation, vehicle speed, engine power, and exhaust temperature are also shown in Figure 4. The dashed horizontal line in Figure 4 is the PMP PCRF-corrected

dx.doi.org/10.1021/es403578b | Environ. Sci. Technol. 2014, 48, 1779−1786

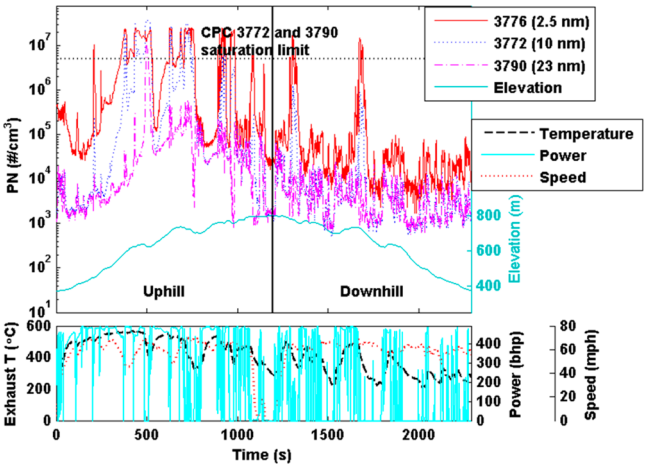

Figure 4. Real-time PN concentrations downstream of the PMP for the on-road flow-of-traffic test.

saturation limit of CPC 3772_10 and CPC 3790_23. Above this saturation limit, the concentrations of CPC 3772_10 and CPC 3790_23 are underestimated. CPC 3772_10 and CPC 3790_23 reached their saturation limits during some time periods of uphill driving. CPC 3776_2.5 was under its saturation limit throughout the entire test.

The CPC 3776_2.5 concentrations were always higher than the CPC 3772_10 and CPC 3790_23 concentrations for the uphill driving, which was expected and consistent with the UDDS results. CPC 3772_10 and CPC 3790_23 agreed well at the beginning of uphill driving. As the test proceeded to t = ~250 s, however, the CPC 3772_10 concentrations gradually increased to levels well above those of CPC 3790_23 and to levels that were closer to those of CPC 3776_2.5, indicating that nucleated particles had grown to particle sizes above 10 nm. In fact, at several times between about 350 and 500 s, the number measured by CPC 3772_10 reached essentially the same level as that indicated by CPC 3776_2.5, indicating that the entire mode had grown above 10 nm and was almost certainly spilling over into the range above 23 nm.

This phenomenon was examined using model distributions. Figure S3 of the Supporting Information shows a model size distribution consisting of two log-normal modes, a nucleation mode representing nucleation and growth downstream of the volatile particle remover (VPR) and an accumulation mode representing true solid particles. Figure S4 of the Supporting Information shows a conceptual model in which the nucleation mode is growing by condensation. As the mode shifts to the right, it grows beyond 10 nm into the counting range of the 10 nm cut-point CPC and eventually into that of the 23 nm CPC. Figure S5 of the Supporting Information shows the count that would be registered by the CPCs as the nucleation mode grows by condensation, first leading to detection by the 10 nm CPC and eventually by the 23 nm CPC. Because solid particles according to the PMP are defined as those detected by the 23 nm CPC, in this example, it could lead to count levels more than 5 times the true solid particle count. The results shown in Figure 4 exhibit behavior similar to the modeling distributions in terms of the CPC counts relative to one another. The model illustrated in Figure S5 of the Supporting Information suggests that, at conditions where the 2.5 and 10 nm CPCs agree, there is already spillover of volatile particles into the counting range of the 23 nm CPC.

Exhaust temperatures in this time window (~350 and 500 s) were even higher than the highest temperatures reached in the UDDS, and again, sulfate formation and/or release of stored sulfates are likely to be driving nucleation and growth by condensation particles downstream of the PMP system but, in this case, into the size range above 10 nm. This is consistent with the large nucleation mode particle concentrations measured by the EEPS in the CVS, which ranged from 1.0×10^7 to 3.6×10^7 particles/cm^3 for particles smaller than 30 nm (see Figure S6 of the Supporting Information). Once this period of elevated condensation was over, CPC 3772_10 and CPC 3790_23 tracked well again from around t = 750 s through the end of the entire test, except for a few other time periods where conditions favoring nucleation downstream of the PMP system occurred.

The downhill driving test cycle usually showed smaller differences between CPC 3776_2.5, CPC 3772_10, and CPC 3790_23, indicating little nucleation downstream of the PMP. Two periods of downstream nucleation were observed for the downhill driving segment shown in Figure 4, one at ~1300 s and one at ~1670 s. The first nucleation peak can be attributed to the truck accelerating up to driving speed after the vehicle turned around at the top of the hill. The second nucleation peak appears to be related to a short uphill segment that occurred during the course of the downhill driving segment, as seen from the elevation in Figure 4. It should be noted that these two periods occurred in only three of the four repeats of the on-road, uphill, and downhill driving tests, leading to relatively large variations for the integrated CPC_3776_2.5 and CPC 3772_10 concentrations, as discussed in section 3.2.

Real-time PN concentrations downstream of the PMP system for the cruise cycle are shown in Figure 5. The real-

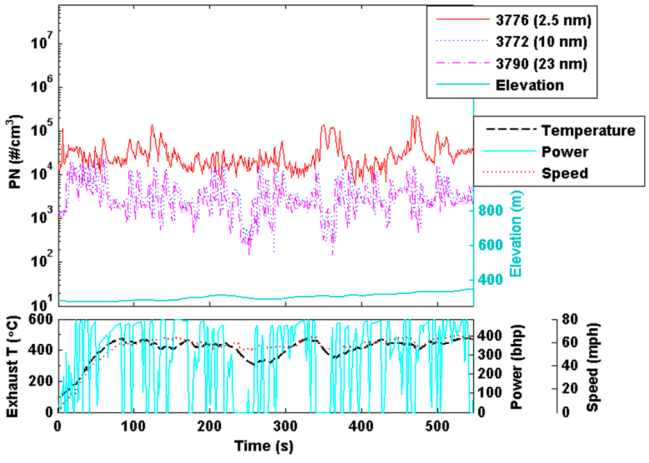

Figure 5. Real-time PN concentrations downstream of the PMP for the cruise on-road test.

time PN concentrations below the PMP show relatively consistent trends, with CPC 3776_2.5 having concentrations about twice those of CPC 3772_10 and CPC 3790_23, with a range from 13 to 100% higher. The CPC 3772_10 and CPC 3790_23 concentrations were very similar throughout the cruise test, indicating negligible particles between 10 and 23 nm. The cruise cycle did not show any periods of significant condensational growth, such as those that were found for the UDDS and uphill cycles. Particle size distributions in the CVS for the cruise on-road test are shown in Figure S7 of the Supporting Information. It shows intermittent burst of

dx.doi.org/10.1021/es403578b | Environ. Sci. Technol. 2014, 48, 1779−1786

nucleation mode from time to time but to much less extent compared to that of uphill driving conditions shown in Figure S6 of the Supporting Information.

3.2. M_{IPSD} and SPN Emissions. The M_{IPSD} and SPN emissions for the UDDS and on-road tests are shown in Figure 6. Note that the left y axis (SPN emissions) is on a logarithmic scale, while the right y axis (M_{IPSD} emissions) is on a linear scale, to improve the readability of the figure. It should be noted that, for the SPN emissions, an outlier was identified for the on-road, flow-of-traffic test using Dixon's Q test[29] at a 95% confidence limit (Q = 0.87 versus a limit value of 0.83). This outlier was excluded from the calculations presented in this paper.

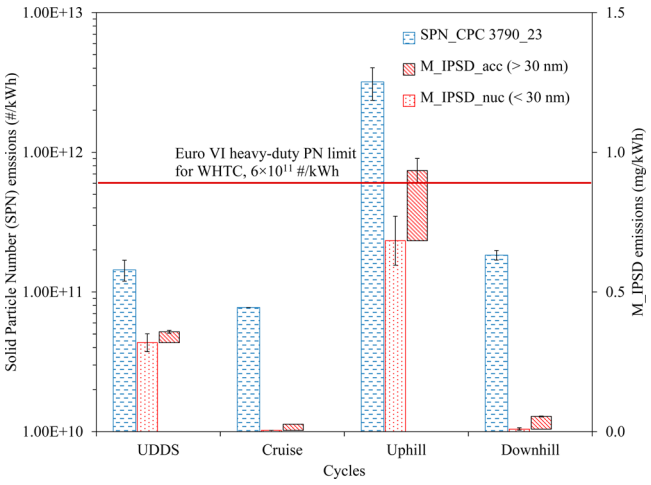

Figure 6. M_{IPSD} and SPN emissions over the on-road and UDDS tests. The left y axis (SPN emissions) is on a logarithmic scale, and the right y axis (M_{IPSD} emissions) is on a linear scale.

Total M_{IPSD} emissions are composed of nucleation mode particles (<30 nm) and accumulation mode particles (>30 nm). Total M_{IPSD} emissions were dominated by the nucleation mode particles for the UDDS and on-road uphill driving tests and by the accumulation mode particles for the on-road downhill driving and cruise driving. The dominance of nucleation mode particles for the UDDS and uphill driving conditions is most likely due to oxidation of SO_2 to SO_3 at high exhaust temperatures, as discussed above. The uphill driving showed higher M_{IPSD}_nuc than the UDDS, as high levels of nucleation occurred throughout the uphill driving (see Figure 4), while for the UDDS cycle, nucleation was predominantly seen between 600 and 780 s, when the exhaust temperature and load was the highest. The total M_{IPSD} for the cruise and downhill driving tests was considerably less than that for the uphill and UDDS cycles. This is due to the lack of nucleation mode particles for the cruise and downhill driving, as well as higher accumulation mode particle emissions for the UDDS and uphill driving. It should be noted that some of the EEPS channels in the nucleation mode size range were saturated during the UDDS and uphill driving conditions of the on-road test. In other words, the M_{IPSD} emissions of nucleation mode particles for the UDDS and uphill driving conditions were underestimated.

Total M_{IPSD} emissions for both the UDDS and on-road tests were more than 6 times lower than the U.S. 2007 heavy-duty PM mass standard, 13.4 mg/kWh. This is consistent with a previous study using the same engine and aftertreatment system.[8] Total M_{IPSD} emissions for the UDDS test were ~6 times higher than those from the downhill driving and cruise driving conditions but ~3 times lower than those from the uphill driving conditions.

SPN emissions of particles larger than 23 nm for the UDDS, downhill driving, and cruise driving were ~3 times lower than the Euro 6 heavy-duty SPN limit for the transient cycle (i.e., WHTC), 6×10^{11} particles/kWh. On the other hand, SPN emissions of particles larger than 23 nm for the uphill driving conditions were ~5 times higher than the Euro 6 SPN limit. It should be noted that the uphill driving conditions here are much more aggressive than the operation during the WHTC. The high exhaust temperatures during the uphill driving conditions probably burned off most of the soot layer that normally aids in particle filtration, thus reducing filtration efficiency and allowing for more solid particles to be emitted. In addition, very high sulfate concentrations under these conditions likely overloaded the VPR, leading to the formation of volatile particles larger than 23 nm and causing solid particle emissions to be overestimated.

It is generally known that the SPN versus PM (on the basis of filter mass) relationship does not exist for diesel emissions with high efficiency diesel particulate filters (DPFs). Andersson et al.[2] reported that SPN varied ~1000 times, while PM varied

Table 1. Calculation Result of the PN_{Acc} versus M_{IPSD_Acc} Relationship from Prior Studies in Comparison to the Result of SPN versus M_{IPSD_Acc} from the Current Study

	test	PN_{Acc}, d_{cutoff} (number/cm³, nm)	M_{IPSD_Acc} (mg/cm³)	PN_{Acc}/M_{IPSD}	reference
vehicle 1, Baseline	UDDS	3.8×10^6, 30	1.0×10^{-6}	3.8×10^{12}	27
vehicle 1, CRT1	UDDS	3.8×10^3, 40	1.6×10^{-9}	2.5×10^{12}	27
vehicle 1, V-SCRT	UDDS	1.2×10^3, 35	9.1×10^{-10}	1.3×10^{12}	27
vehicle 1, Z-SCRT	UDDS	5.1×10^3, 30	3.9×10^{-9}	1.3×10^{12}	27
vehicle 2, DPX	UDDS	2.4×10^3, 40	1.4×10^{-9}	1.8×10^{12}	27
vehicle 3, Horizon	UDDS	9.4×10^2, 30	5.5×10^{-10}	1.7×10^{12}	27
vehicle 4, CCRT	UDDS	1.5×10^3, 30	5.6×10^{-10}	2.7×10^{12}	27
CRT[a]	32% engine load	8.7×10^2, 30	4.7×10^{-10}	1.8×10^{12}	29
		SPN (number/kWh)	M_{IPSD_Acc} (mg/kWh)	SPN/M_{IPSD}	
heavy-duty truck	UDDS	1.44×10^{11}	3.89×10^{-2}	3.71×10^{12}	this study
	cruise	7.75×10^{10}	2.21×10^{-2}	3.51×10^{12}	this study
	downhill	1.84×10^{11}	4.51×10^{-2}	4.07×10^{12}	this study
	uphill	3.19×10^{12}	2.51×10^{-1}	1.27×10^{13}	this study

[a]BP15 fuel, 32% engine load (600 N•m, 1500 rpm).

dx.doi.org/10.1021/es403578b | Environ. Sci. Technol. 2014, 48, 1779−1786

~10 times in their heavy-duty vehicle interlaboratory exercise. They attributed this to adsorption artifacts with the gravimetric PM measurement.

SPN, M_{IPSD_Acc} (Acc means accumulation mode), and SPN/M_{IPSD_Acc} values for this study are presented in Table 1. SPN/M_{IPSD} for UDDS, cruise, and downhill conditions of this study were 3.5×10^{12}, 3.7×10^{12}, and 4.1×10^{12} particles/mg, respectively. However, the SPN/M_{IPSD} value was an order of magnitude higher at 1.3×10^{13} particles/mg for the uphill condition. This can be attributed to the influence of renucleated particles that have grown to particles larger than 23 nm and are counted as SPN. Making reasonable assumptions about the geometric mean diameter (DGN) by number, sigma, and density of accumulation mode particles gives slopes ranging from 1 to 3×10^{12} particles/mg, which is consistent with the results reported here. Particle size distributions from heavy-duty diesel vehicles for two other studies were also used to calculate PN_{Acc}/M_{IPSD_Acc} to compare to the findings of this study. Gross et al.[30] used a CRT with ULSD, and Herner et al.[28] studied a variety of conditions, including baseline with no DPF and different kinds of DPFs along with additional aftertreatment systems, such as diesel oxidation catalysts (DOCs) and/or selective catalytic reductions (SCRs). The Herner et al.[28] baseline result with no DPF gave the highest PN_{Acc}/M_{IPSD_Acc} value. Note PN_{Acc} was used instead of SPN, because SPN was not measured by Gross et al.[30] and Herner et al.[28] PN_{Acc} was determined by integrating the particle size distribution for either the larger than 30 nm particles or the particles larger than the diameter of inflection point (which is larger than 30 nm), depending upon the shape of the particle size distribution. The PN_{Acc}/M_{IPSD_Acc} value ranged from 1.3 to 3.8×10^{12} for the Herner et al.[28] and Gross et al.[30] studies for all other conditions with DPFs and other aftertreatment systems. These results are consistent with the result reported in this study within a factor of 2. These results in Table 1 also agree well with those by Giechaskiel et al.[4] They reported SPN/PM values from 1 to 4×10^{12} particles/mg, but because of the artifact contribution for the filter measurement, the linearity for the SPN/PM relationship was good only for PM emission levels larger than 3 mg/km (mg/kWh). The linearity of the results from this study, on the other hand, was not adversely affected at low particle emissions. Using the IPSD method avoids filter artifacts, such as those reported by Andersson et al.[5] This topic requires further study to better understand the M_{IPSD} (or PM) and SPN relationship at low PM levels and for a wider range of vehicles.

■ ASSOCIATED CONTENT

Supporting Information

Discussion of test repeatability, particle size distributions in the CVS for the UDDS test (Figure S1), average engine loads and average exhaust temperatures for the on-road and UDDS tests (Figure S2), model size distribution downstream of the VPR showing modes (Figure S3), model size distributions downstream of the VPR showing growing nucleation mode (Figure S4), apparent solid number concentrations measured by 3, 10, and 23 nm cut-point diameter CPCs during the growth of DGN of nucleation mode from 3 to 23 nm (Figure S5), particle size distributions in the CVS for the uphill and downhill on-road flow-of-traffic test (Figure S6), particle size distributions in the CVS for the cruise on-road test (Figure S7), SPN and IPSD PM mass emissions on a distance basis (Figure S8), and COVs for the average loads, average exhaust temperatures, PN emissions of particles larger than 23, 10, and 2.5 nm, total M_{IPSD} emissions, M_{IPSD_Acc}, and M_{IPSD_Nuc} for both the on-road and UDDS tests (Figure S9). This material is available free of charge via the Internet at http://pubs.acs.org.

■ AUTHOR INFORMATION

Corresponding Author

*Telephone: 951-781-5742. Fax: 951-781-5790. E-mail: heejung@engr.ucr.edu.

Notes

The authors declare no competing financial interest.

■ ACKNOWLEDGMENTS

The authors acknowledge the CARB for funding (08-302) and lending instruments for this study. The authors gratefully acknowledge AVL List GmbH, Inc. for providing an APC and technical support.

■ GLOSSARY

SPN	solid particle number
PM	particulate matter
UDDS	urban dynamometer driving schedule
IPSD	integrated particle size distribution
M_{IPSD}	particulate matter mass calculated from integrated particle size distribution
CE-CERT	College of Engineering, Center for Environmental Research and Technology
PMP	Particle Measurement Programme
WHSC	world harmonized steady cycle
WHTC	world harmonized transient cycle
PEMS	portable emission measurement system
CVS	constant volume sampling
CRT	continuously regenerating trap
UCR	University of California Riverside
MEL	Mobile Emission Laboratory
APC	AVL particle counter
PCRF	particle concentration reduction factor
CPC	condensation particle counter
EEPS	engine exhaust particle sizer
CARB	California Air Resources Board
VPR	volatile particle remover
DGN	geometric mean diameter by number
ULSD	ultralow sulfur diesel
DPF	diesel particulate filter
DOC	diesel oxidation catalyst
SCR	selective catalytic reduction
ILCE_HD	PMP heavy-duty interlaboratory correlation exercise
COV	coefficient of variation

■ REFERENCES

(1) EPA, EPA/600/8-90/057F, May 2002, Health Assessment Document for Diesel Engine Exhaust.

(2) Andersson, J.; Mamakos, A.; Giechaskiel, B.; Carriero, M.; Martini, G. *Particle Measurement Programme (PMP) Heavy-Duty Interlaboratory Correlation Exercise (ILCE_HD) Final Report*; United Nations Economic Commission for Europe (UNECE): Geneva, Switzerland, 2010.

(3) Giechaskiel, B.; Chirico, R.; DeCarlo, P. F.; Clairotte, M.; Adam, T.; Martini, G.; Heringa, M. F.; Richter, R.; Prevot, A. S. H.; Baltensperger, U.; Astorga, C. Evaluation of the Particle Measurement Programme (PMP) protocol to remove the vehicles' exhaust aerosol volatile phase. *Sci. Total Environ.* **2010**, *408* (21), 5106−5116.

(4) Giechaskiel, B.; Mamakos, A.; Andersson, J.; Dilara, P.; Martini, G.; Schindler, W.; Bergmann, A. Measurement of automotive non-volatile particle number emissions within the European legislative framework: A review. *Aerosol Sci. Technol.* **2012**, *46* (7), 719−749.
(5) Andersson, J.; Giechaskiel, B.; Muñoz-Bueno, R.; Sandbach, E.; Dilara, P. *Particle Measurement Programme (PMP) Light-Duty Inter-laboratory Correlation Exercise (ILCE_LD) Final Report*; United Nations Economic Commission for Europe (UNECE): Geneva, Switzerland, 2007.
(6) Giechaskiel, B.; Carriero, M.; Martini, G.; Andersson, J. Heavy duty Particle Measurement Programme (PMP): Exploratory work for the definition of the test protocol. *SAE Int. J. Engines* **2009**, *2* (1), 1528−1546.
(7) Herner, J. D.; Robertson, W. H.; Ayala, A. Investigation of ultrafine particle number measurements from a clean diesel truck using the european PMP protocol. *SAE Tech. Pap.* **2007**, DOI: 10.4271/2007-01-1114.
(8) Johnson, K. C.; Durbin, T. D.; Jung, H.; Chaudhary, A.; Cocker, D. R.; Herner, J. D.; Robertson, W. H.; Huai, T.; Ayala, A.; Kittelson, D. Evaluation of the european PMP methodologies during on-road and chassis dynamometer testing for DPF equipped heavy-duty diesel vehicles. *Aerosol Sci. Technol.* **2009**, *43* (10), 962−969.
(9) Zheng, Z.; Johnson, K. C.; Liu, Z.; Durbin, T. D.; Hu, S.; Huai, T.; Kittelson, D. B.; Jung, H. S. Investigation of solid particle number measurement: Existence and nature of sub-23 nm particles under PMP methodology. *J. Aerosol Sci.* **2011**, *42* (12), 883−897.
(10) Zheng, Z.; Durbin, T. D.; Karavalakis, G.; Johnson, K. C.; Chaudhary, A.; Cocker, D. R., III; Herner, J. D.; Robertson, W. H.; Huai, T.; Ayala, A.; Kittelson, D. B.; Jung, H. S. Nature of sub-23 nm particles in the solid particle measurement method: A real time data perspective. *Aerosol Sci. Technol.* **2012**, *46* (7), 886−896.
(11) United Nations Economic Commission for Europe (UNECE). *UNECE Regulation 49, Uniform Provisions Concerning the Measures To Be Taken against the Emission of Gaseous and Particulate Pollutants from Compression-Ignition Engines for Use in Vehicles, and the Emission of Gaseous Pollutants from Positive-Ignition Engines Fuelled with Natural Gas or Liquefied Petroleum Gas for Use in Vehicles*; UNECE: Geneva, Switzerland, 2008.
(12) United Nations Economic Commission for Europe (UNECE). *UNECE Regulation 83, Uniform Provisions Concerning the Approval of Vehicles with Regard to the Emission of Pollutants According to Engine Fuel Requirements*; UNECE: Geneva, Switzerland, 2011.
(13) Rubino, L.; Bonnel, P.; Carriero, M.; Krasenbrink, A. Portable emission measurement system (PEMS) for heavy duty diesel vehicle PM measurement: The European PM PEMS program. *SAE Int. J. Engines* **2010**, *2* (2), 660−673.
(14) Johnson, K. C.; Durbin, T. D.; Cocker, D. R., III; Miller, J. W.; Agama, R. J.; Moynahan, N.; Nayak, G. On-road evaluation of a PEMS for measuring gaseous in-use emissions from a heavy-duty diesel vehicle. *SAE Int. J. Commer. Veh.* **2009**, *1* (1), 200−209.
(15) Johnson, K. C.; Durbin, T. D.; Jung, H.; Cocker, D. R., III; Bishnu, D.; Giannelli, R. Quantifying in-use PM measurements for heavy duty diesel vehicles. *Environ. Sci. Technol.* **2011**, *45* (14), 6073−6079.
(16) Kittelson, D. B.; Watts, W. F.; Johnson, J. P.; Rowntree, C.; Goodier, S.; Payne, M.; Preston, W.; Warrens, C.; Ortiz, M.; Zink, U.; Goersmann, C.; Twigg, M. V.; Walker, A. P. Driving down on-highway particulate emissions. *SAE Tech. Pap.* **2006**, DOI: 10.4271/2006-01-0916.
(17) Lanni, T.; Chaterjee, S.; Conway, R.; Windawi, H.; Rosenblatt, D.; Bush, C.; Lowell, D.; Evans, J.; Mclean, R. Performance and durability evaluation of continuously regenerating particulate filters on diesel powered urban buses at NY city transit. *SAE Tech. Pap.* **2001**, DOI: 10.4271/2001-01-0511.
(18) Liu, Z. G.; Vasys, V. N.; Dettmann, M. E.; Schauer, J. J.; Kittelson, D. B.; Swanson, J. Comparison of strategies for the measurement of mass emissions from diesel engines emitting ultra-low levels of particulate matter. *Aerosol Sci. Technol.* **2009**, *43* (11), 1142−1152.
(19) Maricq, M. M.; Xu, N. The effective density and fractal dimension of soot particles from premixed flames and motor vehicle exhaust. *J. Aerosol Sci.* **2004**, *35* (10), 1251−1274.
(20) Kittelson, D. B.; Watts, W. F.; Johnson, J. H. *Diesel Aerosol Sampling Methodology - CRC E-43*; Department of Mechanical Engineering, University of Minnesota: Minneapolis, MN, 2002.
(21) Ristimaki, J.; Vaaraslhti, K.; Lappi, M.; Keskinen, J. Hydrocarbon condensation in heavy-duty diesel exhaust. *Environ. Sci. Technol.* **2007**, *41* (18), 6397−6402.
(22) Park, K.; Cao, F.; Kittelson, D. B.; McMurry, P. H. Relationship between particle mass and mobility for diesel exhaust particles. *Environ. Sci. Technol.* **2003**, *37* (3), 577−583.
(23) *Perry's Chemical Engineers' Handbook*, 8th ed.; Perry, R. H., Gree, D. W., Eds.; McGraw-Hill Press: New York, 2007.
(24) Ntziachristos, L.; Amanatidis, S.; Samaras, Z.; Giechaskiel, B.; Bergmann, A. Use of a catalytic stripper as an alternative to the original PMP measurement protocol. *SAE Int. J. Fuels Lubr.* **2013**, *6* (2), 532−541.
(25) Cooper, B. J.; Thoss, J. E. Role of NO in diesel particulate emission control. *SAE Tech. Pap.* **1989**, DOI: 10.4271/890404.
(26) Swanson, J. J.; Kittelson, D. B.; Watts, W. F.; Gladis, D. D.; Twigg, M. V. Influence of storage and release on particle emissions from new and used CRTs. *Atmos. Environ.* **2009**, *43* (26), 3998−4004.
(27) Kittelson, D. B.; Watts, W. F.; Johnson, J. P.; Rowntree, C.; Payne, M.; Goodier, S.; Warrens, C.; Preston, H.; Zink, U.; Ortiz, M.; Goersmann, C.; Twigg, M. V.; Walker, A. P.; Caldow, R. On-road evaluation of two diesel exhaust aftertreatment devices. *J. Aerosol Sci.* **2006**, *37* (9), 1140−1151.
(28) Herner, J. D.; Hu, S.; Robertson, W. H.; Huai, T.; Chang, M. C. O.; Rieger, P.; Ayala, A. Effect of advanced aftertreatment for PM and NO_x reduction on heavy-duty diesel engine ultrafine particle emissions. *Environ. Sci. Technol.* **2011**, *45* (6), 2413−2419.
(29) Barnett, V.; Lewis, T. *Outliers in Statistical Data*, 3rd ed.; John Wiley and Sons: Hoboken, NJ, 1994.
(30) Grose, M.; Sakurai, H.; Savstrom, J.; Stolzenburg, M. R.; Watts, W. F., Jr.; Morgan, C. G.; Murray, I. P.; Twigg, M. V.; Kittelson, D. B.; McMurry, P. H. Chemical and physical properties of ultrafine diesel exhaust particles sampled downstream of a catalytic trap. *Environ. Sci. Technol.* **2006**, *40* (17), 5502−5507.